




Article

Genome Mining of α -Pyrone Natural Products from Ascidian-Derived Fungus *Amphichorda felina* SYSU-MS7908

Siwen Yuan ^{1,†}, Litong Chen ^{1,†}, Qilin Wu ¹, Minghua Jiang ¹, Heng Guo ¹, Zhibo Hu ¹, Senhua Chen ^{1,2}, Lan Liu ^{1,2,3,4} and Zhizeng Gao ^{1,2,3,4,*}

¹ School of Marine Sciences, Sun Yat-sen University, Guangzhou 510006, China; yuansw@mail2.sysu.edu.cn (S.Y.); chenlt28@mail2.sysu.edu.cn (L.C.); wuqlin3@mail2.sysu.edu.cn (Q.W.); jiangmh23@mail2.sysu.edu.cn (M.J.); guoh59@mail2.sysu.edu.cn (H.G.); huzhb6@mail2.sysu.edu.cn (Z.H.); chensenh@mail.sysu.edu.cn (S.C.); cesllan@mail.sysu.edu.cn (L.L.)

² Southern Laboratory of Ocean Science and Engineering (Guangdong, Zhuhai), Zhuhai 519000, China

³ Southern Marine Science and Engineering Guangdong Laboratory (Zhuhai), Zhuhai 519000, China

⁴ Pearl River Estuary Marine Ecosystem Research Station, Ministry of Education, Zhuhai 519082, China

* Correspondence: gaozhizeng@mail.sysu.edu.cn

† These authors contributed equally to this work.

Abstract: Culturing ascidian-derived fungus *Amphichorda felina* SYSU-MS7908 under standard laboratory conditions mainly yielded meroterpenoid, and nonribosomal peptide-type natural products. We sequenced the genome of *Amphichorda felina* SYSU-MS7908 and found 56 biosynthetic gene clusters (BGCs) after bioinformatics analysis, suggesting that the majority of those BGCs are silent. Here we report our genome mining effort on one cryptic BGC by heterologous expression in *Aspergillus oryzae* NSAR1, and the identification of two new α -pyrone derivatives, amphichopyrone A (1) and B (2), along with a known compound, udagawanone A (3). Anti-inflammatory activities were performed, and amphichopyrone A (1) and B (2) displayed potent anti-inflammatory activity by inhibiting nitric oxide (NO) production in RAW264.7 cells with IC₅₀ values 18.09 ± 4.83 and 7.18 ± 0.93 μ M, respectively.

Keywords: genome mining; α -pyrone natural products; heterologous expression; *Aspergillus oryzae* NSAR1; anti-inflammatory activity



Citation: Yuan, S.; Chen, L.; Wu, Q.; Jiang, M.; Guo, H.; Hu, Z.; Chen, S.; Liu, L.; Gao, Z. Genome Mining of α -Pyrone Natural Products from Ascidian-Derived Fungus *Amphichorda felina* SYSU-MS7908. *Mar. Drugs* **2022**, *20*, 294. <https://doi.org/10.3390/md20050294>

Academic Editor: Zeinab Khalil

Received: 20 March 2022

Accepted: 26 April 2022

Published: 27 April 2022

Publisher's Note: MDPI stays neutral with regard to jurisdictional claims in published maps and institutional affiliations.



Copyright: © 2022 by the authors. Licensee MDPI, Basel, Switzerland. This article is an open access article distributed under the terms and conditions of the Creative Commons Attribution (CC BY) license (<https://creativecommons.org/licenses/by/4.0/>).

1. Introduction

Fungal natural products are an indispensable source for drug development [1,2]. However, under typical laboratory culture conditions, most of the biosynthetic gene clusters (BGCs) from fungi are “silent”; thus, it becomes increasingly difficult to discover novel natural products. Currently, several genome mining strategies have been reported for activating silent BGCs [3], and heterologous expression of target BGCs in a suitable host is one effective approach. Zhu et al. [4] expressed a cryptic BGC from *Trichoderma harzianum* t-22 in *Aspergillus nidulans* A1145 and successfully isolated several tetronate natural products, such as trihazone A–F. Similarly, Li et al. [5] characterized a cryptic BGC from *A. hancockii* in *A. nidulans* LO8030 and discovered a metabolite with a unique prenylated 6/6/6/5 tetracarboxylic skeleton. The quadruple auxotroph *A. oryzae* NSAR1 is also a frequently-used heterologous host for genome mining of fungal natural products. Recently, Jiang et al. [6] used *A. oryzae* as a heterologous host to express two fungal bifunctional terpene synthases and obtained four terpenes featuring 5-6-7-3-5 ring systems; Yan et al. [7] genome mined four new meroterpenoids, funiculolides A–D, by heterologous expression of a cryptic BGC from *A. funiculosus* CBS 116.56.

Discovering novel secondary metabolites from marine-derived fungi has been our group's long-term research interest [8–11]. The fungus *Amphichorda felina* SYSU-MS7908 was isolated from a marine ascidian *Styelaplicata* and fermentation under standard laboratory

conditions mainly gave meroterpenoids and nonribosomal peptides [12,13]. To probe the biosynthetic potential of *A. felina* SYSU-MS7908, the genome was sequenced by Illumina second-generation sequencing, and the assembled genome was analyzed by the antibiotics and secondary metabolite analysis shell (antiSMASH) [14]. Fifty-six secondary metabolites BGCs were found (Figure S1), suggesting that the fungus has great potential to produce structurally diverse natural products.

Pyrones are six-membered cyclic unsaturated esters exhibiting a broad range of activities, such as antifungal, antibiotic, cytotoxic, immunosuppressive, and phytotoxic (Figure 1) [15–17]. One gene cluster, the *amp* cluster discovered from *A. felina* SYSU-MS7908, shares similarities with the *sol* cluster that is responsible for the biosynthesis of solanapyrone D (Figure 2), an α -pyrone containing natural product [18]. However, we had not observed the production of such metabolites from the wild type of *A. felina* SYSU-MS7908, suggesting that this BGC might be silent. We decided to activate this BGC by heterologous expression in *A. oryzae* NSAR1 as it is a robust host to mine fungal natural products [19–21].

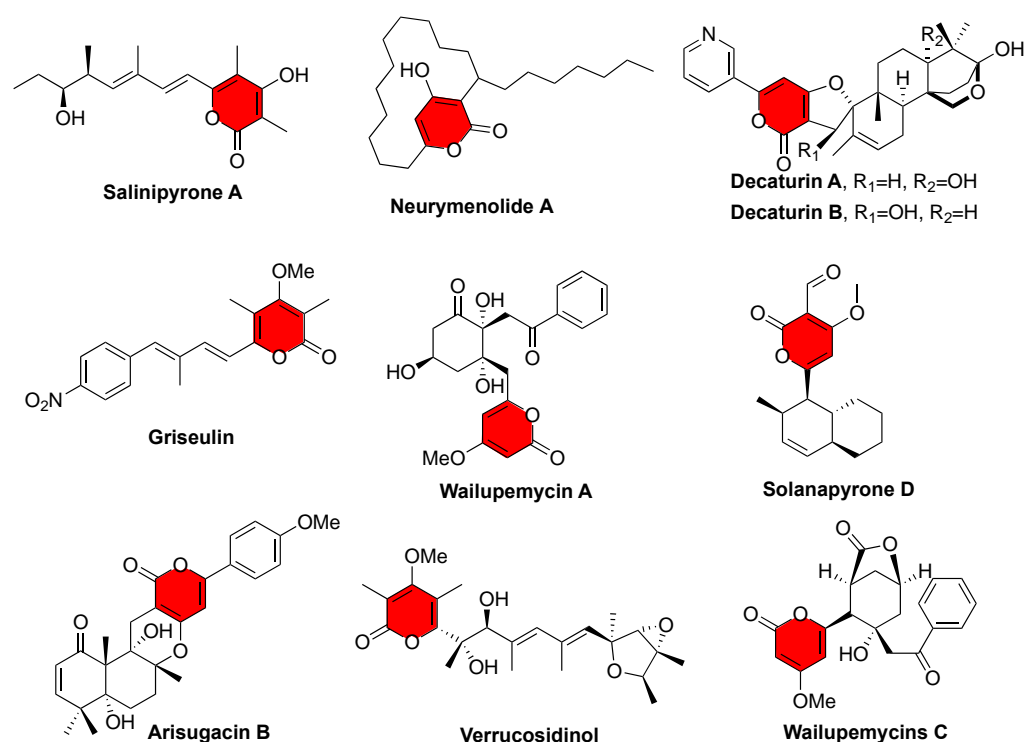


Figure 1. Representative natural products containing α -pyrone motif.

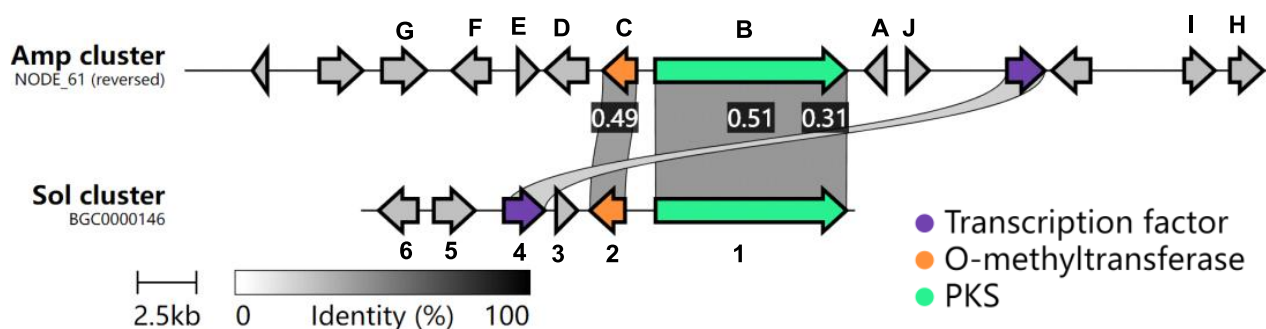


Figure 2. Comparison of the *amp* cluster with the *sol* cluster was performed using the Clinker tool [22].

2. Results and Discussion

2.1. Bioinformatic Analysis of the Amp Cluster

The *amp* cluster contains 10 potential biosynthetic genes (transcription factor and transport excluded, Table 1). AmpB is a polyketide synthase (PKS) that shares 52% protein identity with Sol1 (Figure S2), the PKS involved in solanapyrone D biosynthesis [18,23,24]. AmpC, a putative methyltransferase, shares 49.5% protein identity with Sol2 (Figure S3). Interestingly, no other genes share significant sequence homology between those two clusters (Figure 2), suggesting that the *amp* cluster might produce structurally divergent natural products from solanapyrone D.

Table 1. Proposed functions of open reading frames in the *amp* cluster.

| Amp | AA | Homolog (Accession No.) | S/I ^a (%) | Proposed Function |
|-----|------|-------------------------|----------------------|-------------------------------------|
| A | 285 | - | - | Methyltransferase |
| B | 2633 | Sol1 (D7UQ44.1) | 67.5/51.0 | polyketide synthase |
| C | 455 | Sol2 (XP_045265976.1) | 64.6/49.5 | O-methyltransferase |
| D | 583 | 1A4 (CRG92717.1) | 85.6/72.9 | p450 |
| E | 273 | DltE (XP_045265975.1) | 86.4/72.5 | Oxidoreductase |
| F | 518 | ChyH (XP_037172406.1) | 80.6/67.4 | FAD-linked oxidoreductase |
| G | 487 | — | — | p450 |
| H | 422 | — | — | Unknown |
| I | 398 | — | — | Unknown |
| J | 253 | CsgA (CZT51343.1) | 70.8/52.2 | short-chain dehydrogenase/reductase |

^a Similarity/identity, AA: Amino acid.

2.2. Heterologous Expression of the Amp Cluster in *A. oryzae*

Previous studies suggested that the PKS, Sol1, could produce an advanced biosynthetic intermediate; thus, only the *ampB* gene was introduced into the *A. oryzae* NSAR1 host strain. As expected, the production of amphichopyrone A (**1**) was detected from the expression of the AO-*ampB* construct (Figure 3). With amphichopyrone A (**1**) determined, we next focused on the tailoring genes of the *amp* cluster. AmpC, a putative O-methyltransferase, was then introduced into AO-*ampB* to give the construct AO-*ampBC*. We found that two additional metabolites were produced by AO-*ampBC*. Large-scale fermentation and spectroscopic analyses determined the structures as amphichopyrone B (**2**) and udagawanone A (**3**) [15–17].

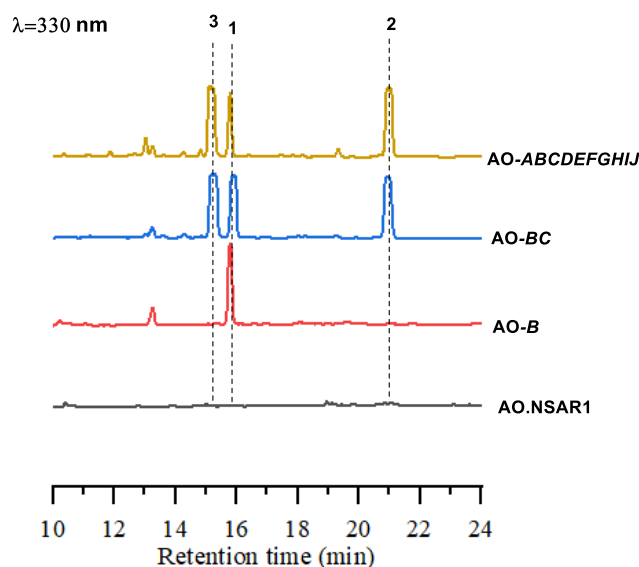


Figure 3. HPLC profiles obtained after expression of respective constructs in *A. oryzae*.

To investigate the final metabolites produced by the *amp* cluster, the remaining eight genes, *ampA*–*ampH*, were included in the construct; unfortunately, the AO-*ampABCDEFGHIJ* construct generated the same product profile as AO-*ampBC* (Figure 3), suggesting amphichopyrone (2) and udagawanone A (3) might be the final products catalyzed by the *amp* cluster (Figure 4). These results suggest that AmpC catalyzed the methylation reaction at C-4 hydroxyl of amphichopyrone A (1) to give amphichopyrone B (2). Hydroxylation of amphichopyrone B (2) to udagawanone A (3) might be catalyzed by endogenous enzymes from *A. oryzae* NSAR1 host (Figure 5).

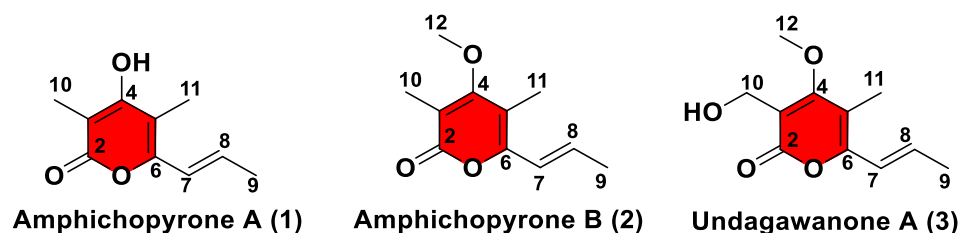


Figure 4. Chemical structures of 1–3.

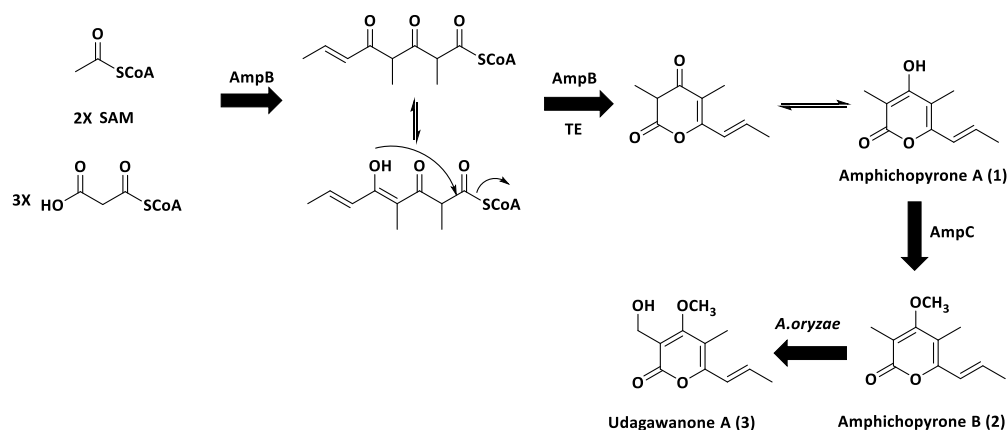


Figure 5. The biosynthetic pathway of 1–3. AmpB is responsible for the formation of amphichopyrone A (1); AmpC introduces a methyl group to give amphichopyrone B (2) by AmpC; hydroxylation of amphichopyrone B (2) to udagawanone A (3) might be catalysed by endogenous enzymes from *A. oryzae* NSAR1 host.

2.3. Characterization of amphichopyrone A (1) and B (2)

Amphichopyrone A (1) was obtained as a white solid. The positive HR-ESI-MS gave an m/z 181.0860 $[M+H]^+$, consistent with the molecular formula $C_{10}H_{13}O_3$ with five degrees of unsaturation (Figure S4). The IR absorption spectrum suggested the presence of hydroxyl (3545 cm^{-1}), conjugated carboxyl ester (1668 cm^{-1}), and olefinic (1568 cm^{-1}) functional groups in the molecule (Figure S5). The UV maxima at approximately 222 and 325 nm suggested the presence of an α -pyrone substructure (Figure S6) [17,25,26]. The ^1H NMR, DEPT NMR, and HSQC experiments showed two olefinic proton signals [δ_{H} 6.42 (1H, dq, $J = 15.4, 1.3\text{ Hz}$)/ δ_{C} 120.6 and 6.50 (1H, dq, $J = 15.4, 6.0\text{ Hz}$)/ δ_{C} 132.0] and three methyls [δ_{H} 1.90 (3H, d, $J = 6.0\text{ Hz}$)/ δ_{C} 17.6; δ_{H} 1.94 (3H, s)/ δ_{C} 8.6 and δ_{H} 2.01 (3H, s)/ δ_{C} 8.5] (Table 2). Except for the above-mentioned five carbons, the ^{13}C NMR spectrum and HSQC experiment revealed the presence of five non-protonated carbons, which were attributed to the 3,4,5,6-tetrasubstituted α -pyrone skeleton (δ_{C} 99.0, 106.3, 151.6, 163.6, 164.3), consisting of one carbonyl carbon and four sp^2 carbons. The HMBC correlations of CH_3 -10 to C-2 (δ_{C} 163.6), C-3 (δ_{C} 99.0) and C-4 (δ_{C} 164.3), CH_3 -11 to C-4 (δ_{C} 164.3), C-5 (δ_{C} 106.3) and C-6 (δ_{C} 151.6), and CH_3 -9 to C-6 (δ_{C} 151.6), C-7 (δ_{C} 120.6) and C-8 (δ_{C} 132.0), which suggested the presence of methyl at C-3 and C-5 site in α -pyrone, and the connection of C-6 site in α -pyrone to the propenyl chain (Figure 6). The coupling constant (15.4 Hz) of two olefinic protons established the *trans* geometric configuration for

$\Delta^{7(8)}$. Hence, the structure of compound **1** was elucidated as (*E*)-4-hydroxy-3,5-dimethyl-6-(prop-1-en-1-yl)-2H-pyran-2-one and named amphichopyrone A (**1**).

Table 2. ^1H (400 MHz) and ^{13}C (100 MHz) NMR data of **1** and **2** in acetone- d_6 .

| No | 1 | | 2 | |
|----|-------------------------------|----------------------------|-------------------------------|----------------------------|
| | δ_{H} (J in Hz) | δ_{C} , Type | δ_{H} (J in Hz) | δ_{C} , Type |
| 2 | | 163.6, C | | 164.5, C |
| 3 | | 99.0, C | | 111.2, C |
| 4 | | 164.3, C | | 168.7, C |
| 5 | | 106.3, C | | 109.4, C |
| 6 | | 151.6, C | | 153.0, C |
| 7 | 6.42, dq (15.4, 1.3) | 120.6, CH | 6.42, dq (15.4, 1.3) | 121.4, CH |
| 8 | 6.50, dq (15.4, 6.0) | 132.0, CH | 6.51, dq (15.4, 6.5) | 133.1, CH |
| 9 | 1.90, d (6.0) | 17.6, CH ₃ | 1.91, d (6.5) | 18.6, CH ₃ |
| 10 | 1.94, s | 8.6, CH ₃ | 1.96, s | 10.4, CH ₃ |
| 11 | 2.01, s | 8.4, CH ₃ | 1.98, s | 9.5, CH ₃ |
| 12 | | | 3.83, s | 60.7, CH ₃ |

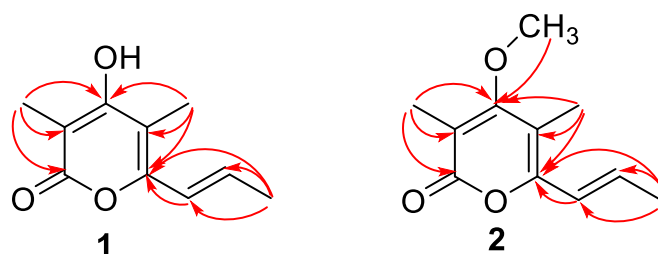


Figure 6. The key HMBC (red arrow) correlations of compounds **1** and **2**.

Amphichopyrone B (**2**) was obtained as a white solid. The molecular formula was determined as $\text{C}_{11}\text{H}_{15}\text{O}_3$ based on the positive HR-ESIMS ions at m/z 195.1019 $[\text{M}+\text{H}]^+$ (calcd. for 195.1016, $\text{C}_{11}\text{H}_{15}\text{O}_3$), suggesting five degrees of unsaturation (Figure S7). The IR absorption bands at 3394, 1668, and 1568 cm^{-1} , indicated the presence of hydroxyl, conjugated carboxyl ester, and olefinic groups in the molecule (Figure S8). Its UV spectrum (λ_{max} 227 and 332 nm) was indicative of the presence of α -pyrone substructure (Figure S9) [18,25,26]. The NMR and HSQC experiments showed two olefinic proton signals [δ_{H} 6.42 (1H, dq, $J = 15.4, 1.3$ Hz)/ δ_{C} 121.4 and 6.51 (1H, dq, $J = 15.4, 6.5$ Hz)/ δ_{C} 133.1] and four methyls [δ_{H} 1.91 (3H, d, $J = 6.5$ Hz)/ δ_{C} 18.6; δ_{H} 1.96 (3H, s)/ δ_{C} 10.4; δ_{H} 1.98 (3H, s)/ δ_{C} 9.5 and δ_{H} 3.83 (3H, s)/ δ_{C} 60.7] (Table 2). Except for the above-mentioned six carbons, the ^{13}C NMR spectrum and HSQC experiment revealed the presence of five non-protonated carbons, which were attributed to the 3,4,5,6-tetrasubstituted α -pyrone skeleton (δ_{C} 109.4, 111.2, 153.0, 164.5, 168.7), consisting of one carbonyl carbon and four sp^2 carbons. The HMBC correlations of CH_3 -10 to C-2 (δ_{C} 164.5), C-3 (δ_{C} 111.2) and C-4 (δ_{C} 168.7), CH_3 -11 to C-4 (δ_{C} 168.7), C-5 (δ_{C} 109.4) and C-6 (δ_{C} 153.0), OCH_3 -12 to C-4 (δ_{C} 168.7) and CH_3 -9 to C-6 (δ_{C} 153.0), C-7 (δ_{C} 121.4) and C-8 (δ_{C} 133.1), which suggested the presence of methyl at C-3 and C-5 site, methoxy at C-4 site in α -pyrone, and the connection of C-6 site in α -pyrone to the propenyl chain (Figure 6). The coupling constant (15.4 Hz) of two olefinic protons established the *trans* geometric configuration for $\Delta^{7(8)}$. Hence, the structure of compound **2** was elucidated as (*E*)-4-methoxy-3,5-dimethyl-6-(prop-1-en-1-yl)-2H-pyran-2-one and named amphichopyrone B (**2**).

2.4. Evaluation of Anti-Inflammatory Activity

Compounds **1–3** were evaluated for in vitro anti-inflammatory activity. Amphichopyrone A (**1**) and B (**2**) displayed potent anti-inflammatory activity by inhibiting LPS-induced NO production with IC_{50} values 18.09 ± 4.83 and $7.18 \pm 0.93\ \mu\text{M}$, respectively. Interestingly, udagawanone A (**3**) shows no activity up to $50\ \mu\text{M}$, suggesting the C-10 hydroxyl group is

detrimental for its anti-inflammatory activity. The pro-inflammatory enzymes, inducible nitric oxide synthase (iNOS) and cyclooxygenase-2 (COX-2), and transcriptional regulators, tumor necrosis factor- α (TNF- α), interleukin-6 (IL-6), and interleukin-1 β (IL-1 β), have been shown to play key roles in inflammatory processes [27,28]. Thus, qPCR experiments were conducted to detect the effect of amphichopyrone B on the activated iNOS, COX-2, TNF- α , IL-6, and IL-1 β . The results showed that the mRNA expression levels of iNOS, COX-2, TNF- α , IL-6, and IL-1 β were down-regulated with the increased concentration of amphichopyrone B (Figure 7), indicating that LPS-induced inflammatory process was inhibited by amphichopyrone B.

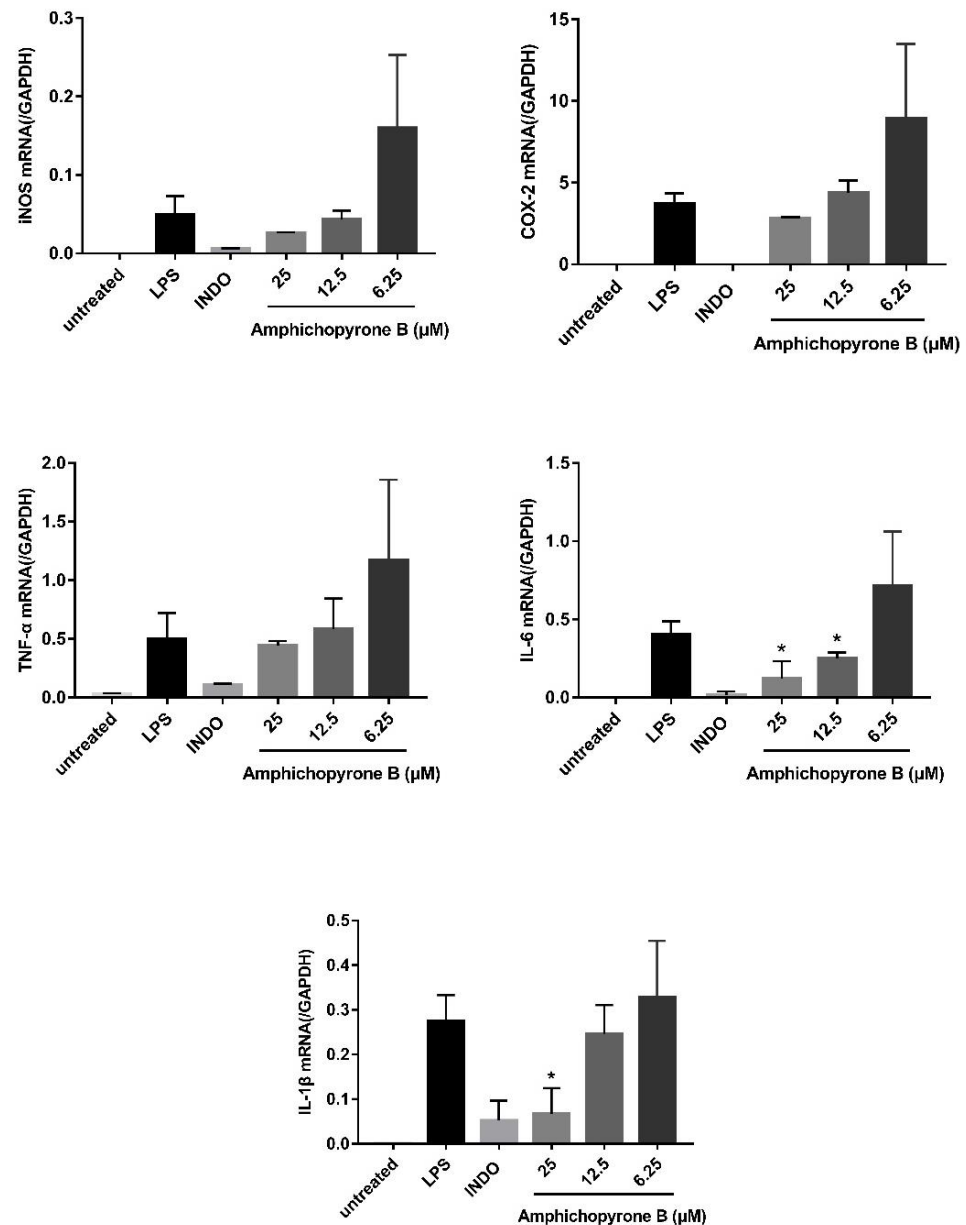


Figure 7. The effect of amphichopyrone B (2) on the LPS-induced iNOS, COX-2, TNF- α , IL-6, and IL-1 β expression. The ‘untreated’ bar is cells only treated with 0.2% DMSO, the ‘LPS’ bar is cells treated with LPS (1 μ g/mL) with 0.2% DMSO, the ‘INDO’ bar is cells treated with indomethacin (50 μ M) together and LPS (1 μ g/mL), and 25 μ M\ 12.5 μ M\ 6.25 μ M represents cells treated with three concentrations of amphichopyrone B (2) together with LPS (1 μ g/mL). The mRNA expression levels of iNOS, COX-2, TNF- α , IL-6, and IL-1 β were down-regulated, suggesting that the LPS-induced inflammatory processes were inhibited by amphichopyrone B. * $p < 0.05$ vs. LPS treatment group.

3. Materials and Methods

3.1. General Materials

Chemicals were purchased from Sangon Biotech Co., Ltd. (Shanghai, China), Thermo Fisher Scientific (Shanghai, China), Sigma-Aldrich Trading Co., Ltd. (Shanghai, China) or J&K Scientific Ltd (Beijing, China), unless noted otherwise. Column Chromatography (CC) was carried out using silica gel (200–300 mesh, Qingdao Marine Chemical Factory, Qingdao, China).

DNA Sequence analysis and primer synthesis were performed by TsingKe Biological Technology Co., Ltd. (Guangzhou, China). Plasmid extraction kits and DNA purification kits were purchased from Tianjin Biotech Co., Ltd. (Beijing, China). PCR analysis was accomplished using a Bio-Rad CFX™ Thermal Cycle with Phanta Super-Fidelity DNA Polymerase (Vazyme, Nanjing, China). The assembly of DNA fragments and the construction of recombinant plasmids were performed by using Clone Express® MultiS One Step Cloning Kit (Vazyme, Nanjing, China). Yatalase™ was purchased from Takara Co., Ltd. (Dalian, China). UV spectra were collected on Waters 2998 photodiode array detector (Waters, Boston, MA, USA). NMR spectra were obtained on a Bruker Avance 400 MHz (Bruker, Switzerland) with tetramethylsilane (TMS) as the internal standard. HR-ESIMS data were measured on a Thermo LCQ DECA XP plus mass spectrometer using a Luna 5u C18 (2) 100A 150 × 4.60 mm 5-micron column (Thermo Scientific, Waltham, MA, USA). The Semi-preparative and analytical HPLC were performed on a Waters 1525 system equipped with a Waters 2998 photodiode array detector (Waters, Boston, MA, USA), using a Welch Ultimate® XB-C18 column (10 mm × 250 mm, 5 μm, Welch Materials, Inc., Shanghai, China) and COSMOSIL 5C18-AR-II column (4.6 mm × 250 mm, 5 μm, Nacalai Tesque, Inc., Kyoto, Japan), respectively. The mobile phases for analytical HPLC were H₂O containing 0.1% formic acid (A) and CH₃CN containing 0.1% formic acid (B), and the gradient elution was 15–80% B (0–15 min), 80–100% B (15–20 min), 100–100% B (20–28 min), 100–15% B (28–30 min), and 15% B (30–33 min) with a flow rate of 1 mL/min.

3.2. Strains and Media

The strain, *Amphichorda felina* SYSU-MS7908, was isolated from a marine ascidian *Styelaplicata* collected from the north atoll of the Xisha Islands, South China Sea, China, in 2018, isolated using the standard protocol [29] and identified by the morphological and the internal transcribed spacer (ITS) of the nuclear ribosomal DNA data analysis (Accession number MT786206). The whole genome sequences of *A. felina* SYSU-MS7908 have been deposited in the GenBank database with an accession number JAEMHR000000000. The sequences of *amp* A–J have been submitted to GenBank (OL906410–OL906419). The proposed functions of *amp* A–J in Table 1 are based on the protein BLAST results. The gene cluster comparison figure between the *amp* and *sol* clusters was generated with the Clinker tools with the corresponding annotated sequence files using default parameters [22]. Primer sequences are listed in Table S1.

The heterologous expression host *Aspergillus oryzae* NSAR1 and corresponding plasmids were gifts from professors Ikuro Abe and Katsuhiko Kitamoto (the University of Tokyo, Tokyo, Japan) [30]. The mycelia of *A. oryzae* strains expressing the respective constructs were inoculated into 10 mL DPY medium (2% dextrin, 1% polypeptide, 0.5% yeast extract, 0.5% KH₂PO₄, 0.05% MgSO₄·7H₂O) and cultured at 28 °C and 220 rpm for 2 days. Then the DPY medium was transferred to the 100 mL modified Czapek-Dox (CD) medium (0.3% NaNO₃, 0.2% KCl, 0.05% MgSO₄·7H₂O, 0.1% KH₂PO₄, 0.002% FeSO₄·7H₂O, 1% polypeptide, 2% starch, pH 5.5), and grown at 28 °C and 220 rpm for 6 days to induce the expression of heterologous genes under the *amyB* promoter.

3.3. Construction of Recombinant Plasmids

To construct the expression plasmids for *A. oryzae*, the genes (*ampA-ampJ*) of the *amp* cluster were first amplified using the genomic DNA of *Amphichorda felina* SYSU-MS7908 as a template. Each amplified DNA fragment was then introduced into the pTAex3 vector [31],

and the gene expression cassette, *amyB* promoter, the target gene, and the *amyB* terminator were amplified from the pTAex3-based plasmid. These gene expression cassettes were then inserted into the HindIII-linearized pPTRI [32], pBARI [33], SpeI-linearized pAdeA [34], and XbaI-linearized pUNA [35]. Plasmids constructed in this study are listed in Table S2.

3.4. Transformation of *A. oryzae* NSAR1

The transformation of *A. oryzae* NSAR1 was conducted via the protoplast–polyethylene glycol method. Mycelia of the parent strain from the solid culture in potato dextrose agar were inoculated in 10 mL DPY medium and cultured at 28 °C and 220 rpm for 2 days, which were then transferred to 100 mL DPY medium and cultured for 24 h. The mycelia were collected by filtration and digested by 1% Yatalase in 0.6 M (NH₄)₂SO₄, 50mM maleic acid, pH 5.5 at 30 °C for 4 h to remove cell walls. The resulting protoplasts were collected by centrifugation at 1500 rpm for 10 min and washed once with Solution 2 (1.2 M sorbitol, 50 mM CaCl₂·2H₂O, 35 mM NaCl, 10M Tris-HCl, pH 7.5). Then, 200 µL protoplast suspension (1 × 10⁷ cells/mL) and about 10 µg plasmids were gently mixed and incubated on ice for 30 min, followed by the addition of 1.3 mL Solution 3 (60% PEG4000, 50 mM CaCl₂·2H₂O, 10 M Tris-HCl, pH 7.5) at three times. After the mixture was placed at room temperature for 20 min, 5 mL Solution 2 was added. Following centrifugation at 1500 rpm for 10 min, the precipitates were suspended in 200 µL of Solution 2 and spread on the bottom selective medium with 0.8% agar, which was then covered with the selective overlay medium containing 1.5% agar. The selective medium was composed of 0.2% NH₄Cl, 0.1% (NH₄)₂SO₄, 0.05% KCl, 0.05% NaCl, 0.1% KH₂PO₄, 0.05% MgSO₄·7H₂O, 0.002% FeSO₄·7H₂O, 2% glucose, 1.2 M sorbitol supplemented with 0.15% methionine, 0.1% arginine, 0.01% adenine, 0.1 µg/mL pyriothiamine hydrobromide and 35 µL/mL glufosinate-ammonium based on the plasmids used. The *A. oryzae* strain containing the *amp* cluster was verified by checking the relevant exogenous target genes using PCR analysis (Figure S10). *A. oryzae* transformants constructed in this study are listed in Table S3.

3.5. Extraction, Isolation, and Characterization

The strain expressing the AO-*ampBC* construct was cultured in a CD-starch medium (3.0 L) at 28 °C and 220 rpm for 5 days. The culture was extracted with ethyl acetate (3 × 3.0 L). The crude extract was subjected to silica column chromatography eluted with CH₂Cl₂-methanol (*v/v*, 100:10). The fraction was purified by RP-HPLC using 55% methanol in water, a flow rate of 3 mL/min, a Welch Ultimate[®] XB-C18 column (10 mm × 250 mm, 5 µm, Welch) to afford three white solids **1** (10 mg), **2** (15 mg), and **3** (14 mg).

3.6. Anti-Inflammatory Activity

The RAW264.7 cells were used to evaluate the anti-inflammatory activity of compounds **1–3** following a literature procedure [36]. The cells were seeded in 96-well plates at a density of 5 × 10⁵ cells/mL. After 12 h, LPS (1 µg/mL) and samples were added to the cells and then incubated for 24 h at 37 °C. The quantity of nitrite accumulated in the culture medium was measured as an indicator of NO production. Then, 50 µL of cell culture medium with 100 µL Griess reagent were mixed and incubated for 10 min at room temperature. The absorbance was determined at 540 nm wavelength with a microplate reader.

3.7. Quantification of the Expression of *iNOS*, *COX-2*, *TNF-α*, *IL-6*, and *IL-1β* and *GAPDH*

The RAW264.7 cells were precultured in 6-well plates at a density of 1.0 × 10⁶ cells/mL for 12 h. The cells were then treated with LPS (1 µg/mL), indomethacin (50 µM) together with LPS (1 µg/mL), three concentrations (6.25, 12.5, 25 µM) of amphichopyrone B (**2**) together with LPS (1 µg/mL) for 24 h at 37 °C under a 5% CO₂ atmosphere. The negative control (untreated group) was treated only with 0.2% DMSO. The total RNA was isolated using the RNeasy kit (TransGen Biotech Co., Ltd., Beijing, China). The FastKing gDNA Dispelling RT SuperMix (TransGen Biotech Co., Ltd., Beijing, China) was used for reverse

transcription at 42 °C for 15 min and 95 °C for 3 min. The BIO-RAD CFX96 Real-Time system (Bio-Rad Laboratories, Inc., Hong Kong, China) and SYBR Green Premix Pro Taq HS qPCR kit (Accurate Biology Co., Ltd., Changsha, China) were used for qPCR amplification of iNOS, COX-2, TNF- α , IL-6, and IL-1 β and GAPDH (40 cycles at 95 °C for 5 s and 60 °C for 30 s).

4. Conclusions

Many genome mining strategies have been reported for activating silent BGCs to produce novel natural products. In this study, we heterologously expressed a cryptic gene cluster from *Amphichorda felina* SYSU-MS7908 in *A. oryzae* NSAR1 and two new metabolites, amphichopyrone A (1) and amphichopyrone B (2), along with a known compound, udagawanone A (3), were isolated. Amphichopyrone A (1) and amphichopyrone B (2) show potent anti-inflammatory activity by inhibiting LPS-induced NO production with IC₅₀ values 18.09 \pm 4.83 and 7.18 \pm 0.93 μ M, respectively.

Supplementary Materials: The following supporting information can be downloaded at: <https://www.mdpi.com/article/10.3390/md20050294/s1>, Table S1: Primers used in this study; Table S2: Plasmids constructed in this study; Table S3: *A. oryzae* transformants constructed in this study; Table S4: ¹H NMR and ¹³C NMR data of; Figure S1: The antiSMASH (fungal version) result of *Amphichorda felina* SYSU-MS7908; Figure S2: The UV spectrum of Amphichopyrone A (1); Figure S3: The UV spectrum of Amphichopyrone B (2); Figure S4: The UV spectrum of udagawanone A (3); Figure S5: The IR spectrum of Amphichopyrone A (1); Figure S6: The IR spectrum of Amphichopyrone B (2); Figure S7: HRESIMS spectrum for Amphichopyrone A (1); Figure S8: HRESIMS spectrum for Amphichopyrone B (2); Figure S9: PCR analysis for the AO-*amp*ABCDEFGHIJ construct.; Figure S10: Amino acid sequence alignment of AmpB with Sol1; NMR Spectra.

Author Contributions: Z.G. and L.L. designed the experiments; S.Y., L.C., Q.W., M.J. and Z.H. performed the experiments; S.C. and H.G. analyzed the data; S.Y. and Z.G. wrote the paper. All authors have read and agreed to the published version of the manuscript.

Funding: This study was supported by Key-Area Research and Development Program of Guangdong Province (2020B1111030005), National Natural Science Foundation of Guangdong (No. 2018A030313334 and 2019A1515011710), Southern Marine Science and Engineering Guangdong Laboratory (Zhuhai) (No. SML2021SP319), the National Natural Science Foundation of China (Grant Nos. U20A2001), and the Open Fund of State Key Laboratory of Applied Optics (SKLAO2020001A10).

Institutional Review Board Statement: Not applicable.

Informed Consent Statement: Not applicable.

Data Availability Statement: Not applicable.

Acknowledgments: We thank Ikuro Abe and Katsuhiko Kitamoto for the quadruple auxotrophic heterologous expression host *Aspergillus oryzae* NSAR1.

Conflicts of Interest: The authors declare no conflict of interest.

References

1. Pham, J.V.; Yilma, M.A.; Feliz, A.; Majid, M.T.; Maffetone, N.; Walker, J.R.; Kim, E.; Cho, H.J.; Reynolds, J.M.; Song, M.C.; et al. A review of the microbial production of bioactive natural products and biologics. *Front. Microbiol.* **2019**, *10*, 1404. [[CrossRef](#)] [[PubMed](#)]
2. Woodruff, H.B. Natural products from microorganisms. *Science* **1980**, *208*, 1225–1229. [[CrossRef](#)] [[PubMed](#)]
3. Rutledge, P.J.; Challis, G.L. Discovery of microbial natural products by activation of silent biosynthetic gene clusters. *Nat. Rev. Microbiol.* **2015**, *13*, 509–523. [[CrossRef](#)] [[PubMed](#)]
4. Zhu, Y.; Wang, J.; Mou, P.; Yan, Y.; Chen, M.; Tang, Y. Genome mining of cryptic tetronate natural products from a PKS-NRPS encoding gene cluster in *Trichoderma harzianum* t-22. *Org. Biomol. Chem.* **2021**, *19*, 1985–1990. [[CrossRef](#)] [[PubMed](#)]
5. Li, H.; Shu, S.; Kalaitzis, J.A.; Shang, Z.; Vuong, D.; Crombie, A.; Lacey, E.; Piggott, A.M.; Chooi, Y.H. Genome mining of *Aspergillus hancockii* unearths cryptic polyketide hancockinone A featuring a prenylated 6/6/6/5 carbocyclic skeleton. *Org. Lett.* **2021**, *23*, 8789–8793. [[CrossRef](#)]

6. Jiang, L.; Zhang, X.; Sato, Y.; Zhu, G.; Minami, A.; Zhang, W.; Ozaki, T.; Zhu, B.; Wang, Z.; Wang, X.; et al. Genome-based discovery of enantiomeric pentacyclic sesterterpenes catalyzed by fungal bifunctional terpene synthases. *Org. Lett.* **2021**, *23*, 4645–4650. [[CrossRef](#)]
7. Yan, D.; Matsuda, Y. Genome mining-driven discovery of 5-methylorsellinate-derived meroterpenoids from *Aspergillus funiculosus*. *Org. Lett.* **2021**, *23*, 3211–3215. [[CrossRef](#)]
8. Chen, S.; Jiang, M.; Chen, B.; Salaenoi, J.; Niaz, S.-I.; He, J.; Liu, L. Penicamide A, a unique N,N'-ketal quinazolinone alkaloid from ascidian-derived fungus *Penicillium* sp. 4829. *Mar. Drugs* **2019**, *17*, 522. [[CrossRef](#)]
9. Chen, S.; Shen, H.; Deng, Y.; Guo, H.; Jiang, M.; Wu, Z.; Yin, H.; Liu, L. Roussoelins A and B: Two phenols with antioxidant capacity from ascidian-derived fungus *Roussoella siamensis* SYSU-MS4723. *Mar. Life Sci. Technol.* **2021**, *3*, 69–76. [[CrossRef](#)]
10. Chen, S.; Shen, H.; Zhang, P.; Cheng, H.; Dai, X.; Liu, L. Anti-glioma trichobamide A with an unprecedented tetrahydro-5H-furo[2,3-b]pyrrol-5-one functionality from ascidian-derived fungus *Trichobotrys effuse* 4729. *Chem. Commun.* **2019**, *55*, 1438–1441. [[CrossRef](#)]
11. Niaz, S.-I.; Zhang, P.; Shen, H.; Li, J.; Chen, B.; Chen, S.; Liu, L.; He, J. Two new isochromane derivatives penisochromanes A and B from ascidian-derived fungus *Penicillium* sp. 4829. *Nat. Prod. Res.* **2019**, *33*, 1262–1268. [[CrossRef](#)] [[PubMed](#)]
12. Jiang, M.H.; Wu, Z.E.; Wu, Q.L.; Yin, H.M.; Guo, H.; Yuan, S.W.; Liu, Z.M.; Chen, S.H.; Liu, L. Amphichoterpenoids A-C, unprecedented picoline-derived meroterpenoids from the ascidian-derived fungus *Amphichorda felina* SYSU-MS7908. *Chin. Chem. Lett.* **2021**, *32*, 1893–1896. [[CrossRef](#)]
13. Liang, M.; Lyu, H.N.; Ma, Z.Y.; Li, E.W.; Cai, L.; Yin, W.B. Genomics-driven discovery of a new cyclodepsipeptide from the guanophilic fungus *Amphichorda guana*. *Org. Biomol. Chem.* **2021**, *19*, 1960–1964. [[CrossRef](#)] [[PubMed](#)]
14. Weber, T.; Blin, K.; Duddela, S.; Krug, D.; Kim, H.U.; Brucoleri, R.; Lee, S.Y.; Fischbach, M.A.; Müller, R.; Wohlleben, W.; et al. antiSMASH 3.0—a comprehensive resource for the genome mining of biosynthetic gene clusters. *Nucleic Acids Res.* **2015**, *43*, W237–W243. [[CrossRef](#)] [[PubMed](#)]
15. Lee, J. Recent Advances in the synthesis of 2-pyrones. *Mar. Drugs* **2015**, *13*, 1581–1620. [[CrossRef](#)]
16. McGlacken, G.P.; Fairlamb, I.J. 2-Pyrone natural products and mimetics: Isolation, characterisation and biological activity. *Nat. Prod. Rep.* **2005**, *22*, 369–385. [[CrossRef](#)]
17. Macabeo, A.P.G.; Cruz, A.J.C.; Narmani, A.; Arzanlou, M.; Babai-Ahari, A.; Pilapil, L.A.E.; Garcia, K.Y.M.; Huch, V.; Stadler, M. Tetrasubstituted α -pyrone derivatives from the endophytic fungus, *Neurospora udagawae*. *Phytochem. Lett.* **2020**, *35*, 147–151. [[CrossRef](#)]
18. Kasahara, K.; Miyamoto, T.; Fujimoto, T.; Oguri, H.; Tokiwano, T.; Oikawa, H.; Ebizuka, Y.; Fujii, I. Solanapyrone synthase, a possible Diels-Alderase and iterative type I polyketide synthase encoded in a biosynthetic gene cluster from *Alternaria solani*. *ChemBioChem* **2010**, *11*, 1245–1252. [[CrossRef](#)]
19. Zhang, W.Y.; Zhong, Y.; Yu, Y.; Shi, D.F.; Huang, H.Y.; Tang, X.L.; Wang, Y.H.; Chen, G.D.; Zhang, H.P.; Liu, C.L.; et al. 4-Hydroxy pyridones from heterologous expression and cultivation of the native host. *J. Nat. Prod.* **2020**, *83*, 3338–3346. [[CrossRef](#)]
20. Guo, J.; Cai, Y.S.; Cheng, F.; Yang, C.; Zhang, W.; Yu, W.; Yan, J.; Deng, Z.; Hong, K. Genome mining reveals a multiproduct sesterterpenoid biosynthetic gene cluster in *Aspergillus ustus*. *Org. Lett.* **2021**, *23*, 1525–1529. [[CrossRef](#)]
21. Wang, W.-G.; Du, L.-Q.; Sheng, S.-L.; Li, A.; Li, Y.-P.; Cheng, G.-G.; Li, G.-P.; Sun, G.; Hu, Q.-F.; Matsuda, Y. Genome mining for fungal polyketide-diterpenoid hybrids: Discovery of key terpene cyclases and multifunctional P450s for structural diversification. *Org. Chem. Front.* **2019**, *6*, 571–578. [[CrossRef](#)]
22. Gilchrist, C.L.M.; Chooi, Y.H. Clinker & clustermap.js: Automatic generation of gene cluster comparison figures. *Bioinformatics* **2021**, *37*, 2473–2475.
23. Kim, W.; Park, J.-J.; Gang, D.R.; Peever, T.L.; Chen, W. A novel type pathway-specific regulator and dynamic genome environments of a solanapyrone biosynthesis gene cluster in the fungus *Ascochyta rabiei*. *Eukaryot. Eukaryot. Cell* **2015**, *14*, 1102–1113. [[CrossRef](#)] [[PubMed](#)]
24. Kim, W.; Park, C.-M.; Park, J.-J.; Akamatsu, H.O.; Peever, T.L.; Xian, M.; Gang, D.R.; Vandemark, G.; Chen, W. Functional analyses of the Diels-Alderase gene sol5 of *Ascochyta rabiei* and *Alternaria solani* indicate that the solanapyrone phytotoxins are not required for pathogenicity. *Mol. Plant-Microbe Interact.* **2015**, *28*, 482–496. [[CrossRef](#)]
25. Fujimoto, H.; Satoh, Y.; Yamazaki, M. Four new immunosuppressive components, Kobiin and Kobifuranones A, B, and C, from an *Ascomycete*, *Gelasinospora kobei*. *Chem. Pharm. Bull.* **1998**, *46*, 211–216. [[CrossRef](#)]
26. Fujimoto, H. Immunomodulatory constituents from *Ascomycetous* fungi. *J. Nat. Med.* **2018**, *72*, 20–31. [[CrossRef](#)]
27. Sun, L.D.; Wang, F.; Dai, F.; Wang, Y.H.; Lin, D.; Zhou, B. Development and mechanism investigation of a new piperlongumine derivative as a potent anti-inflammatory agent. *Biochem. Pharmacol.* **2015**, *95*, 156–169. [[CrossRef](#)]
28. Xue, G.M.; Li, X.Q.; Chen, C.; Chen, K.; Wang, X.B.; Gu, Y.C.; Luo, J.G.; Kong, L.Y. Highly oxidized guaianolide sesquiterpenoids with potential anti-inflammatory activity from *Chrysanthemum indicum*. *J. Nat. Prod.* **2018**, *81*, 378–386. [[CrossRef](#)]
29. Kjer, J.; Debbab, A.; Aly, A.H.; Proksch, P. Methods for isolation of marine-derived endophytic fungi and their bioactive secondary products. *Nat. Protoc.* **2010**, *5*, 479–490. [[CrossRef](#)]
30. Jin, F.J.; Maruyama, J.; Juvvadi, P.R.; Arioka, M.; Kitamoto, K. Development of a novel quadruple auxotrophic host transformation system by *argB* gene disruption using *adeA* gene and exploiting adenine auxotrophy in *Aspergillus oryzae*. *FEMS Microbiol. Lett.* **2004**, *239*, 79–85. [[CrossRef](#)]

31. Fujii, T.; Yamaoka, H.; Gomi, K.; Kitamoto, K.; Kumaga, C. Cloning and nucleotide sequence of the ribonuclease T1 gene (*rntA*) from *Aspergillus oryzae* and its expression in *Saccharomyces cerevisiae* and *Aspergillus oryzae*. *Biosci. Biotechnol. Biochem.* **1995**, *59*, 1869–1874. [[CrossRef](#)] [[PubMed](#)]
32. Kubodera, T.; Yamashita, N.; Nishimura, A. Pyrithiamine resistance gene (*ptrA*) of *Aspergillus oryzae*: Cloning, characterization and application as a dominant selectable marker for transformation. *Biosci. Biotechnol. Biochem.* **2000**, *64*, 1416–1421. [[CrossRef](#)] [[PubMed](#)]
33. Pall, M.L.; Brunelli, J.P. A series of six compact fungal transformation vectors containing polylinkers with multiple unique restriction sites. *Fungal Genet. Newsl.* **1993**, *40*, 59–62. [[CrossRef](#)]
34. Jin, F.J.; Maruyama, J.-I.; Juvvadi, P.R.; Arioka, M.; Kitamoto, K. Adenine auxotrophic mutants of *Aspergillus oryzae*: Development of a novel transformation system with triple auxotrophic hosts. *Biosci. Biotechnol. Biochem.* **2004**, *68*, 656–662. [[CrossRef](#)] [[PubMed](#)]
35. Yamada, O.; Lee, B.R.; Gomi, K.; Iimura, Y. Cloning and functional analysis of the *Aspergillus oryzae* conidiation regulator gene *brlA* by its disruption and misscheduled expression. *J. Biosci. Bioeng.* **1999**, *87*, 424–429. [[CrossRef](#)]
36. Li, H.; Zhang, Q.; Jin, X.; Zou, X.; Wang, Y.; Hao, D.; Fu, F.; Jiao, W.; Zhang, C.; Lin, H.; et al. Dysifragilone A inhibits LPS induced RAW264.7 macrophage activation by blocking the p38 MAPK signaling pathway. *Mol. Med. Rep.* **2018**, *17*, 674–682. [[CrossRef](#)]